Auto-Calibrating Wave-CS for Motion-Robust Accelerated MRI

Feiyu Chen[1], Tao Zhang[1,2], Joseph Y. Cheng[1,2], John M. Pauly[1], and Shreyas S. Vasanawala[2]

[1]Electrical Engineering and [2]Radiology, Stanford University, Stanford, California, United States

Purpose: Wave-encoding[1] has been demonstrated to improve the performance of accelerated MRI reconstruction by distributing the under-sampling in both phase-encode and readout directions. Wave-CS[2] combines wave-encoding with compressed sensing and has been shown to significantly reduce aliasing artifacts in brain imaging. However, a separate calibration scan is required. Subject motion between the calibration scan and the wave-encoded acquisition may introduce sensitivity variation and therefore degrade image quality. In this work, we propose a motion-robust auto-calibrating Wave-CS technique for abdominal and pelvic imaging.

Methods: The concept is to use the wave-encoded center k-space and the known point-spread-function (PSF) of wave-encoding to reconstruct a Cartesian central k-space for calibration. In detail, the wave-modulated signal and the Cartesian signal has the following relationship in the k_x-y-z domain[1]:

$$S_{wave}[k_x, y, z] = Psf[k_x, y, z] \cdot S_{Cartesian}[k_x, y, z]$$

The PSF can be expressed as:

$$Psf[k_x, y, z] = \exp(-i\gamma \int (g_y(\tau)y + g_z(\tau)z)d\tau)$$

$$= \exp(C_1 \cdot y + C_2 \cdot z) = \exp(C_1 \cdot \Delta y \cdot i_y + C_2 \cdot \Delta z \cdot i_z)$$

where C_1 and C_2 are constants associated with gradients g_y and g_z, y *and* z are positions in image space, Δy and Δz are the corresponding spatial resolutions, and i_y and i_z are spatial indices. The wave-encoded central k-space can be treated as an independent low-resolution k-space modulated by the same PSF with lower resolution. Thus, by replacing Δy and Δz with $\Delta y_{calib} = \frac{N_y}{N_{y,calib}} \cdot \Delta y$, and $\Delta z_{calib} = \frac{N_z}{N_{z,calib}} \cdot \Delta z$, where N_y, N_z are the acquisition matrix size, and $N_{y,calib}$, $N_{z,calib}$ are the calibration size, we can obtain a set of low-resolution PSF (Fig.1b), and subsequently reconstruct the Cartesian central k-space using inverse Fourier transform of the PSF. The resulted Cartesian center can then be used for calibration.

To test the accuracy of this approach, five phantom experiments with both fully sampled Cartesian acquisition and wave-encoded acquisition were conducted. The normalized root-mean-square-error (RMSE) between low-resolution images from the calibration data in Cartesian acquisition and those reconstructed by the proposed method were calculated as an indicator of calibration accuracy (Fig. 2). Two volunteer scans (Figs. 3 and 4) were acquired on a 3T GE MR750 scanner (GE Healthcare, Waukesha, WI) with wave encoding (3 cycles of sinusoids, 4mT/m amplitude) using a 32-channel cardiac coil (Invivo Corp., Gainesville, FL) and a 32-channel torso array coil (NeoCoil, Pewaukee, WI), respectively. In the

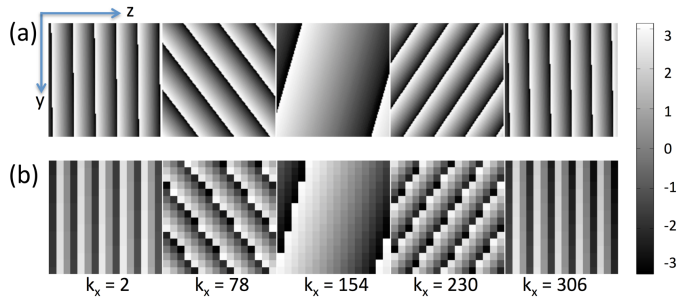

Fig.1 *(a) Phase of the full-size PSF displayed in the y-z plane in [-π, π] for kx = 2, 78, 154, 230, and 306; (b) Phase of the corresponding low-resolution PSF for the 16(y)×16(z) calibration region.*

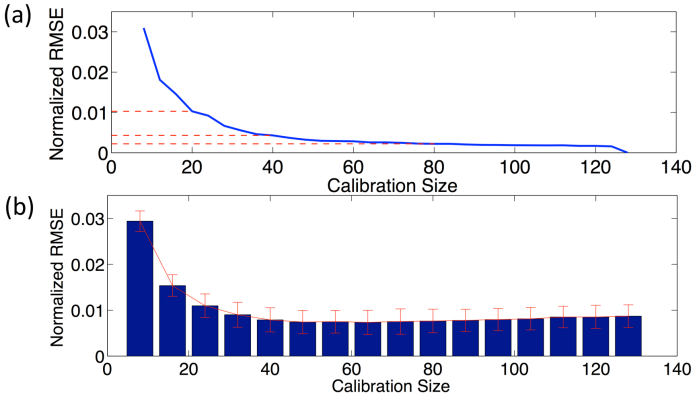

Fig.2 *Normalized RMSE for low-resolution calibrating data decreases while size of calibration kspace increases, as shown in: (a) simulated wave-encoded kspace with an accurate PSF, and (b) five phantom experiments with estimated PSFs.*

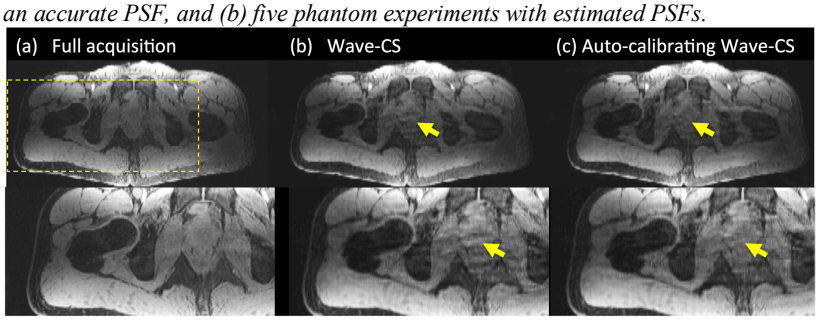

Fig.3 *Comparison of reconstructed images using full acquisition (a), Wave-CS (b), and the auto-calibrating Wave-CS (c) during free breathing scans at a reduction factor of 5.1. 1.5x zoomed-in images are shown in the second row. Yellow arrows point the major difference between these reconstructions.*

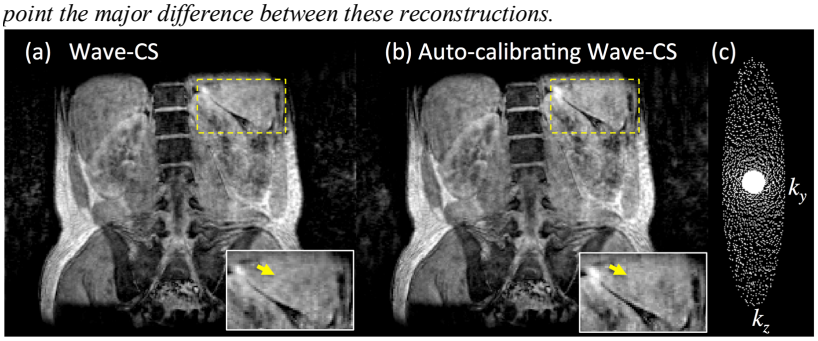

Fig.4 *Comparison of reconstructed images using conventional Wave-CS (a) and auto-calibrating Wave-CS (b) with breath-held acquisitions at a reduction factor of 6.2. Conventional Wave-CS (a) uses a separated breath-hold calibration scan to achieve the coil sensitivity maps. 1.5x zoomed-in images are shown at the bottom right corners. Yellow arrows point the major difference between these reconstructions. The VDRad sampling mask is shown in (c).*

second scan, spatial selective excitations in frequency-encoding directions were used to maintain a reasonable over-sampling factor of ~1.5. Down sampling using a VDRad trajectory[3] was simulated (Fig. 3) and implemented (Fig. 4) in a 3D SPGR sequence with a 16×16 calibration region at a reduction factor of 5.1 and 6.2, respectively. Sensitivity maps were estimated using ESPIRiT[4] from Cartesian acquisition directly and from wave-encoded acquisition with the proposed method. CS-SENSE reconstruction using the same sampling pattern was implemented for the auto-calibrating method and compared with the conventional Wave-CS method. Acquisition parameters for the 3D SPGR sequence were: TR/TE 12/2.2ms, FA 15°, and BW $\pm$ 125kHz. Acquisition matrices were 308(k_x)×128(k_y)×128(k_z) (with partial readout factor 0.6) for FOV 420mm (R/L)×210mm (A/P)×210mm (S/I), and 256(k_x)×256(k_y)×64(k_z) for FOV 400mm (S/I)×400mm (R/L)×256mm (A/P).

Results: Normalized RMSE for low-resolution calibrating images decreases with increased size of calibration for the auto-calibrating method (Fig. 2). Artifacts due to motion and under-sampling occur in both reconstructions (Fig. 3). Auto-calibrating Wave-CS reduces the artifacts in both free breathing and breath-holding cases, in comparison with conventional Wave-CS approach (Figs. 3 and 4).

Discussion: To maintain a low RMSE of less than 2%, a calibration size of ~20×20 is necessary. Using larger calibration size would be helpful until the calibration size reaches 40×40. When the calibration size is larger than 40×40, the non-zero RMSE is mainly caused by inaccurate PSF estimation of wave encoding. In comparison with conventional Wave-CS, the proposed auto-calibration approach can reduce the motion artifacts and the aliasing artifacts due to sensitivity variations between the calibration and the wave-encoded acquisitions, as pointed by yellow arrows in Figs. 3 and 4. As the acquisition parameters were designed for post-contrast T1 weighted acquisitions, the image quality may improve in clinical contrast-enhanced scans.

Conclusion: In this work, we evaluated the feasibility of auto-calibrating Wave-CS for potential applications with subject motion. Applying this method in dynamic contrast enhanced abdominal imaging will be our future work.

References:

1. Bilgic B, et al. Wave-CAIPI for highly accelerated 3D imaging. Magn. Reson. Med. 2015, 73(6): 2152-2162.

2. Curtis A, et al. Wave-CS: Combining wave encoding and compressed sensing. Proc. Intl. Soc. Mag. Reson. Med. 2015, 23: 0082.

3. Cheng JY, et al. Free-breathing pediatric MRI with nonrigid motion correction and acceleration, Journal of Magnetic Resonance Imaging, 2014, 42(2): 407-420.

4. Uecker M, et al. ESPIRiT-an eigenvalue approach to autocalibrating parallel MRI: where SENSE meets GRAPPA. Magn. Reson. Med. 2014, 71(3): 990-1001.

Acknowledgements:

We gratefully acknowledge the support of the Tashia and John Morgridge Faculty Scholars Fund, NIH/NIBIB R01 EB009690, R01 EB019241, and GE Healthcare.